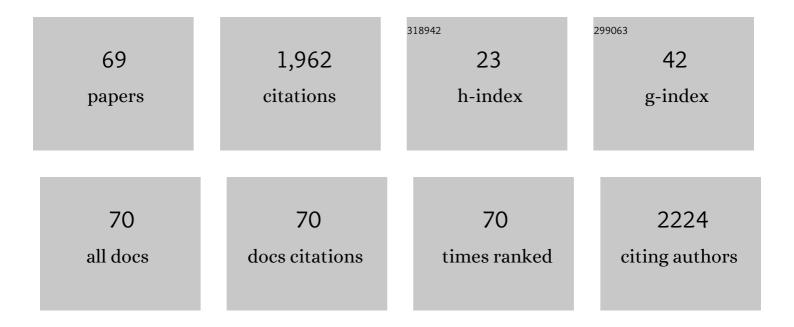
List of Publications by Year in descending order

Source: https://exaly.com/author-pdf/1056179/publications.pdf Version: 2024-02-01



#	Article	IF	CITATIONS
1	The promotion of sulfuric vacancy in two-dimensional molybdenum disulfide on the sensing performance of SF6 decomposition components. Applied Surface Science, 2022, 571, 151377.	3.1	10
2	Highly adjustable piezoelectric properties in two-dimensional LiAlTe ₂ by strain and stacking. Nanotechnology, 2022, 33, 055702.	1.3	4
3	Laser In-Situ synthesis of metallic cobalt decorated porous graphene for flexible In-Plane microsupercapacitors. Journal of Colloid and Interface Science, 2022, 610, 775-784.	5.0	10
4	Laser In Situ Preparation of S-Doped Porous Graphene for Flexible Microsupercapacitors. IEEE Electron Device Letters, 2022, 43, 327-330.	2.2	3
5	Indium Selenide/Antimonene Heterostructure for Multifunctional Optoelectronics. IEEE Transactions on Electron Devices, 2022, 69, 1155-1161.	1.6	8
6	The piezoelectricity of 2D Janus ZnBrI: Multiscale prediction. Chemical Physics Letters, 2022, 794, 139506.	1.2	6
7	Metal Oxides/Carbon Felt Pressure Sensors with Ultraâ€Broadâ€Range High Sensitivity. Advanced Materials Interfaces, 2022, 9, .	1.9	10
8	Polyaniline Modified Laser-Scribed Graphene for High-Performance Microsupercapacitors. IEEE Electron Device Letters, 2022, 43, 966-969.	2.2	6
9	Ultrasensitive and self-alarm pressure sensor based on laser-induced graphene and sea urchin-shaped Fe2O3 sandwiched structure. Chemical Engineering Journal, 2022, 448, 137664.	6.6	17
10	Graphene-based film heater fabricated by laser writing. Materials Letters, 2021, 284, 128869.	1.3	11
11	Monolayer h-BN/C3B lateral heterostructures with promising electronic and optical properties: A first-principles study. Chemical Physics, 2021, 541, 111042.	0.9	2
12	Monolayer Janus Te ₂ Se-based gas sensor to detect SO ₂ and NO _x : a first-principles study. Physical Chemistry Chemical Physics, 2021, 23, 1675-1683.	1.3	19
13	Theoretical investigations of novel Janus Pb ₂ SSe monolayer as a potential multifunctional material for piezoelectric, photovoltaic, and thermoelectric applications. Nanoscale, 2021, 13, 15611-15623.	2.8	12
14	Low-temperature Sintering of Cu/functionalized Multi-walled Carbon Nanotubes Composite Paste for Power Electronic Packaging. IEEE Transactions on Power Electronics, 2021, , 1-1.	5.4	3
15	A C ₂ N/ZnSe heterostructure with type-II band alignment and excellent photocatalytic water splitting performance. New Journal of Chemistry, 2021, 45, 13571-13578.	1.4	10
16	Sea urchin-like microstructure pressure sensors with an ultra-broad range and high sensitivity. Nature Communications, 2021, 12, 1776.	5.8	109
17	Piezoelectricity of Janus Sb2Se2Te monolayers: A first-principles study. Journal of Applied Physics, 2021, 129, .	1.1	26
18	Gas Sensor Based on Semihydrogenated and Semifluorinated h-BN for SFâ,† Decomposition Components Detection. IEEE Transactions on Electron Devices, 2021, 68, 1878-1885.	1.6	12

#	Article	IF	CITATIONS
19	Giant Piezoelectricity of Janus Mâ,,SeX (M = Ge, Sn; X = S, Te) Monolayers. IEEE Electron Device Letters, 2021, 42, 561-564.	2.2	25
20	High sensitive and selective toxic gas sensor based on monolayer Tetra-MoN2 for sensing NO: A first-principles study. Chemical Physics Letters, 2021, 769, 138359.	1.2	4
21	A heterostructure of C3N/h-BN with effectively regulated electronic properties by E-field and strain. Chemical Physics Letters, 2021, 770, 138461.	1.2	5
22	Optimal Cu paste thickness for large-area Cu-Cu joint. Materials Letters, 2021, 291, 129533.	1.3	3
23	Facile and Scalable Fabrication of High-Performance Microsupercapacitors Based on Laser-Scribed <i>In Situ</i> Heteroatom-Doped Porous Graphene. ACS Applied Materials & Interfaces, 2021, 13, 22426-22437.	4.0	35
24	Monolayer square-Ag2X (XÂ=ÂS, Se): Excellent n-type thermoelectric materials with high power factors. Applied Surface Science, 2021, 550, 149230.	3.1	4
25	One-step laser fabrication of phosphorus-doped porous graphene electrodes for high-performance flexible microsupercapacitor. Carbon, 2021, 180, 56-66.	5.4	59
26	Type-II AsP/Sc2CO2 van der Waals heterostructure: an excellent photocatalyst for overall water splitting. International Journal of Hydrogen Energy, 2021, 46, 32882-32892.	3.8	23
27	A novel Hf2CO2/WS2 van der Waals heterostructure as a potential candidate for overall water splitting photocatalyst. Materials Science in Semiconductor Processing, 2021, 133, 105947.	1.9	17
28	PbSnSâ,,-Based Gas Sensor to Detect SFâ,† Decompositions: DFT and NEGF Calculations. IEEE Transactions on Electron Devices, 2021, 68, 5322-5325.	1.6	13
29	SWCNT-bridged laser-induced graphene fibers decorated with MnO2 nanoparticles for high-performance flexible micro-supercapacitors. Carbon, 2021, 183, 128-137.	5.4	43
30	Laser synthesis of superhydrophilic O/S co-doped porous graphene derived from sodium lignosulfonate for enhanced microsupercapacitors. Journal of Power Sources, 2021, 513, 230558.	4.0	36
31	2D β-tellurene: Increase sensitivity toward toxic cyanide molecules. Vacuum, 2021, 194, 110619.	1.6	5
32	Facile fabrication of rGO/LIG-based temperature sensor with high sensitivity. Materials Letters, 2021, 304, 130637.	1.3	23
33	Properties-enhanced gas sensor based on Cu-doped tellurene monolayer to detect acetone molecule: a first-principles study. Molecular Physics, 2021, 119, .	0.8	6
34	Sc2CF2/Janus MoSSe heterostructure: A potential Z-scheme photocatalyst with ultra-high solar-to-hydrogen efficiency. International Journal of Hydrogen Energy, 2021, 46, 39830-39843.	3.8	34
35	Porous ZnO/rGO Nanosheetâ€Based NO ₂ Gas Sensor with High Sensitivity and ppb‣evel Detection Limit at Room Temperature. Advanced Materials Interfaces, 2021, 8, 2101511.	1.9	18
36	Novel Braceletlike BiSbX ₃ (X = S, Se) Monolayers with an In-Plane Negative Poisson's Ratio and Anisotropic Photoelectric Properties. Journal of Physical Chemistry Letters, 2021, 12, 11353-11360.	2.1	4

#	Article	IF	CITATIONS
37	The ultralow thermal conductivity and ultrahigh thermoelectric performance of fluorinated Sn2Bi sheet in room temperature. Nano Energy, 2020, 67, 104283.	8.2	16
38	Graphene oxide humidity sensor with laser-induced graphene porous electrodes. Sensors and Actuators B: Chemical, 2020, 325, 128790.	4.0	74
39	Tellurene Nanoflake-Based NO ₂ Sensors with Superior Sensitivity and a Sub-Parts-per-Billion Detection Limit. ACS Applied Materials & Interfaces, 2020, 12, 47704-47713.	4.0	54
40	Enhancing power factor of SnSe sheet with grain boundary by doping germanium or silicon. Npj Computational Materials, 2020, 6, .	3.5	9
41	A Monolayer Composite of h-BN Doped by a Nano Graphene Domain: As Sensitive Material for SO ₂ Gas Detection. IEEE Electron Device Letters, 2020, 41, 1404-1407.	2.2	18
42	Controlling information duration on rewritable luminescent paper based on hybrid antimony (III) chloride/small-molecule absorbates. Science Advances, 2020, 6, .	4.7	61
43	Integrated Sensing and Warning Multifunctional Devices Based on the Combined Mechanical and Thermal Effect of Porous Graphene. ACS Applied Materials & Interfaces, 2020, 12, 53049-53057.	4.0	16
44	Capacitance creep and recovery behavior of magnetorheological elastomers. Journal of Intelligent Material Systems and Structures, 2020, , 1045389X2096991.	1.4	2
45	Tellurene based biosensor for detecting DNA/RNA nucleobases and amino acids: A theoretical insight. Applied Surface Science, 2020, 532, 147451.	3.1	27
46	High sensitivity gas sensor to detect SF6 decomposition components based on monolayer antimonide phosphorus. Chemical Physics Letters, 2020, 756, 137868.	1.2	20
47	Two-dimensional penta-SiAs ₂ : a potential metal-free photocatalyst for overall water splitting. Journal of Materials Chemistry C, 2020, 8, 11980-11987.	2.7	24
48	Health Monitoring and Automatic Notification Device Based on Laser-Induced Graphene. IEEE Transactions on Electron Devices, 2020, 67, 4488-4492.	1.6	2
49	An investigation of the positive effects of doping an Al atom on the adsorption of CO ₂ on BN nanosheets: a DFT study. Physical Chemistry Chemical Physics, 2020, 22, 9368-9374.	1.3	22
50	Promoting Crystal Distribution Uniformity Based on the CVD Method with the Aid of Finite Element Methods. Crystal Growth and Design, 2020, 20, 777-782.	1.4	3
51	Improved Performance of Flexible Graphene Heater Based on Repeated Laser Writing. IEEE Electron Device Letters, 2020, 41, 501-504.	2.2	26
52	Flexible laser-induced-graphene omnidirectional sound device. Chemical Physics Letters, 2020, 745, 137275.	1.2	15
53	Monolayer Tellurene-Based Gas Sensor to Detect SF ₆ Decompositions: A First-Principles Study. IEEE Electron Device Letters, 2019, 40, 1522-1525.	2.2	44
54	PCF-Graphene: A 2D sp ² -Hybridized Carbon Allotrope with a Direct Band Gap. Journal of Physical Chemistry C, 2019, 123, 4567-4573.	1.5	29

#	Article	IF	CITATIONS
55	Symmetry-breaking induced large piezoelectricity in Janus tellurene materials. Physical Chemistry Chemical Physics, 2019, 21, 1207-1216.	1.3	134
56	Single-layer BiOBr: An effective <i>p</i> -type 2D thermoelectric material. Journal of Applied Physics, 2019, 125, .	1.1	22
57	Ultralow lattice thermal conductivity induced high thermoelectric performance in the δ-Cu ₂ S monolayer. Nanoscale, 2019, 11, 10306-10313.	2.8	43
58	Bi2O2Se nanosheet: An excellent high-temperature n-type thermoelectric material. Applied Physics Letters, 2018, 112, .	1.5	94
59	2D carbon sheets with negative Gaussian curvature assembled from pentagonal carbon nanoflakes. Physical Chemistry Chemical Physics, 2018, 20, 9123-9129.	1.3	6
60	A new porous metallic silicon dicarbide for highly efficient Li-ion battery anode identified by targeted structure search. Carbon, 2018, 140, 680-687.	5.4	25
61	Three-dimensional pentagonal silicon: Stability and properties. Computational Materials Science, 2018, 155, 373-377.	1.4	8
62	Cu S superionic compounds: Electronic structure and thermoelectric performance enhancement. Journal of Alloys and Compounds, 2017, 722, 17-24.	2.8	21
63	Recent advances in 2D thermoelectric materials. Proceedings of SPIE, 2016, , .	0.8	4
64	Lattice thermal conductivity of penta-graphene. Carbon, 2016, 105, 424-429.	5.4	120
65	Assembling π-Conjugated Molecules with Negative Gaussian Curvature for Efficient Carbon-Based Metal-Free Thermoelectric Material. Journal of Physical Chemistry C, 2016, 120, 27829-27833.	1.5	7
66	A new C=C embedded porphyrin sheet with superior oxygen reduction performance. Nano Research, 2015, 8, 2901-2912.	5.8	35
67	Thermoelectric properties of single-layered SnSe sheet. Nanoscale, 2015, 7, 15962-15970.	2.8	256
68	Stability and properties of 2D porous nanosheets based on tetraoxa[8]circulene analogues. Nanoscale, 2014, 6, 14962-14970.	2.8	27
69	CuInSe2 ultrathin nanoplatelets: novel self-sacrificial template-directed synthesis and application for flexible photodetectors. Chemical Communications, 2012, 48, 9162.	2.2	63